BEAM DYNAMICS STUDIES IN THE SuperKEKB LINEAR ACCELERATOR AND BEAM TRANSPORT SYSTEM*

A. Aguirre †, I. Agapov, Deutsches Elektronen-Synchrotron DESY, Hamburg, Germany
N. Iida, T. Mori, High Energy Accelerator Research Organization, Tsukuba, Japan

Abstract

Achieving the next luminosity milestone at SuperKEKB requires improved *emittance preservation of the injected beams*, currently limited by the injector chain. While emittance growth in the LINAC and beam-transport (BT) lines has been studied, the combined impact of collective effects, lattice imperfections, and field non-idealities remains unclear. Key contributions include *horizontal emittance growth from incoherent and coherent synchrotron radiation (ISR and CSR)*, particularly in the electron beam transfer line (BTe), as well as additional dilution from short-range wakefields and alignment errors. Magnetic-field measurements of the BTe dipoles also reveal non-ideal profiles that must be considered. This study integrates wakefields, ISR/CSR, realistic alignment errors, and updated BTe dipole fields within a unified tracking framework to quantify their combined effect on emittance growth.

INTRODUCTION

SuperKEKB [1] collides asymmetric-energy electrons and positrons at the $\Upsilon(4S)$ resonance, enabling precision measurements of time-dependent CP violation in $B\bar{B}$ decays. The facility targets a peak luminosity of 6×10^{35} cm^{-2} s^{-1}; as of March 2026 a record of 5.24×10^{34} cm^{-2} s^{-1} has been reached, with 1×10^{35} cm^{-2} s^{-1} as the next operational milestone. Reaching this goal relies on the nano-beam scheme [2], which demands ultra-low emittance beams. The injector [3] consists of a LINAC followed by a positron damping ring, with two ~500 m beam transport (BT) lines delivering beams to the low-energy ring (LER) and high-energy ring (HER). Emittance preservation throughout this chain is therefore critical. Several mechanisms degrade beam quality in transport: short-range wakefields, coherent and incoherent synchrotron radiation (CSR/ISR) [5], magnetic field imperfections, and alignment errors. The BTe is of particular concern due to its bending geometry and measured dipole field deviations. This paper quantifies the individual and combined impact of these effects on emittance growth and injection performance.

BEAM DYNAMICS IN THE LINAC AND BEAM TRANSFER LINES

All simulations presented in this contribution were performed using OCELOT [6]. A lattice converter from SAD [7] to OCELOT was developed [8] to enable these studies. SuperKEKB linac comprises two accelerating sections of 120 m and 500 m joined by a 180-degree arc, accelerating electrons to 7 GeV at the entrance of the beam transfer line. The optics and layout are shown in Fig. 1. The same tunnel also serves positron injection, though the present study considers electron beam operation only.

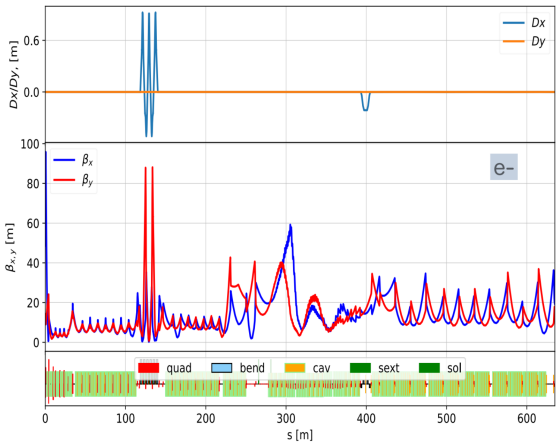

Figure 1: Optics and layout of the SuperKEKB linac injector.

The physics effects taken into account in simulations include space charge in the low-energy sections, longitudinal and transverse wakefields, and incoherent (ISR) and coherent (CSR) synchrotron radiation in the arc. Due to present uncertainty in phase-space distribution, an initial Gaussian bunch profile is assumed; longitudinal phase-space reconstruction at the gun exit is ongoing [9], and will be incorporated in future simulations.

Space charge We evaluated space charge effects assuming an initial Gaussian beam at the gun, with a beam energy of 8.26 MeV as indicated by recent measurements. Although recent measurements suggest a bunch length of 5 mm, results for 1 mm and 3 mm are also presented for comparison. Two bunch charges of 2 nC and 3 nC were considered, along with two values of initial normalized emittance, $\varepsilon_{n,i} = 10$ and 20 mm · mrad, corresponding to possible real values from downstream emittance measurements in same sector. Beam was tracked to the entrance of the first accelerating cavity; results in are summarized in Table 1.

Short-range wakefields In wakefield studies we begin tracking from SECTOR A (~8 m downstream of the gun), where beam measurements provide well-defined initial parameters. Wakefields are implemented via a tabulated longitudinal wake $W(s)$, computed analytically using the empirical model for disk-loaded structures [10]:

$$\mathscr{W}(s) = -\int_0^\infty W(s')\,\lambda_z(s-s')\,ds', \qquad (1)$$

* This work was supported by The Europe-America-Japan Accelerator Development Exchange Programme (EAJADE), a Marie Sklodowska-Curie Research and Innovation Staff Exchange (SE) action, funded by the EU under Horizon-Europe Grant agreement ID: 101086276
† andrea.aguirre.polo@desy.de

Table 1: Final Transverse Normalized Beam Emittances in mm·mrad

$\varepsilon_{n,i}$ [mm·mrad]	Charge [nC]	σ_z [mm]	ε_{xn}	ε_{yn}
10.0	2.0	1	21.009	17.362
		3	12.491	11.554
		5	11.139	10.739
	3.0	1	28.368	22.617
		3	14.744	12.973
		5	12.159	11.345
20.0	2.0	1	27.069	24.538
		3	21.467	20.932
		5	20.720	20.498
	3.0	1	33.211	28.692
		3	22.869	21.761
		5	21.292	20.824

where the single-particle wake is given by

$$W(s) = \frac{Z_0 c}{\pi a^2} \exp\left(-\sqrt{s/s_1}\right), \qquad (2)$$

with $s_1 = 0.41\, a^{1.8} g^{1.6} / p^{2.4}$. The S-band disk-loaded cavities are characterised by a cell period $p = \lambda/3 = 35.0\,\text{mm}$, an iris radius a of 10.5 mm, and a gap length $g \approx 29.2\,\text{mm}$. Figure 2 shows the longitudinal phase space at the linac exit with and without wakefields at an RF phase of 3° (the energy-spread-minimizing setting for 2 nC). The wakefield case (red) exhibits a visible energy chirp relative to the unperturbed distribution (blue), confirming that collective effects are non-negligible at this operating point.

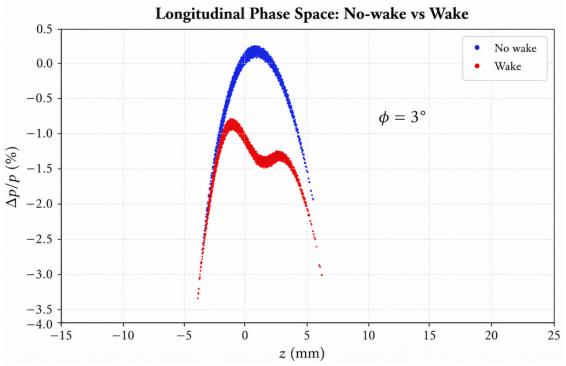

Figure 2: Longitudinal phase space at the end of the linac without (blue) and with (red) short-range wakefields, for an RF phase of 3° and a bunch charge of 2 nC.

Transverse wakefields The transverse dipole wake for the same disk-loaded structure is given by the Bane–Stupakov empirical model [10]:

$$W_x(s) = \frac{4 Z_0 c\, s_2}{\pi a^4} \left[1 - \left(1 + \sqrt{s/s_2}\right) e^{-\sqrt{s/s_2}}\right], \qquad (3)$$

where $s_2 = 0.17\, a^{1.79} g^{0.38} / p^{1.17}$. In OCELOT transverse wakes are computed from the longitudinal wakefield expansion via the Panofsky–Wenzel theorem. To this end, we need to provide the h_{13} and h_{24} coefficients, defined as

$$h_{13}(s) = h_{24}(s) = \frac{1}{2}\frac{d}{ds} W_x(s) = -\frac{Z_0 c}{\pi a^4} e^{-\sqrt{s/s_2}}, \qquad (4)$$

where the equality $h_{13} = h_{24}$ holds for a rotationally symmetric structure.

Electron beam trajectory Accurate modelling of transverse wakefield effects requires a realistic beam trajectory through the linac. Real-time BPM readings were used to reconstruct the actual trajectory in both planes to assign a transverse offset (d_x, d_y) to each accelerating cavity, as shown in Fig. 3. Offsets reach up to ~1 mm; this orbit is used as the reference trajectory up to section C, where wire scanner data are available for comparison.

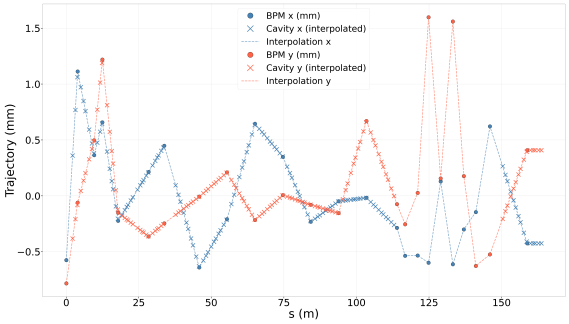

Figure 3: Beam trajectory along the linac reconstructed from BPM readings (circles), with linear interpolation (dashed) evaluated at each cavity position (crosses), in the horizontal (top) and vertical (bottom) planes.

Simulations including only transverse wakefield effects yield an emittance growth of approximately 40 µm. Random quadrupoles misalignments with rms amplitudes of 50, 100, and 150 µm result in the values of 21, 38, and 57 µm rad.

Electron beam particle distribution Including all collective effects simultaneously, longitudinal and transverse short-range wakefields together with CSR, we tracked 100,000 particles at 2.5 nC through the full beamline up to the J-Arc exit. The resulting 6D phase space (Fig. 4) shows a pronounced x-δ correlation, a non-Gaussian horizontal profile, and the characteristic wakefield energy chirp in the longitudinal plane, while the vertical plane remains well-preserved.

Electron beam Transfer Line The BTe line delivers 7 GeV electrons through two achromatic sections, BT1 and BT2, to the High-Energy Ring. A persistent challenge is significant horizontal emittance growth between these sections. Figure 5 shows the optical and longitudinal beam dynamics parameters along the BTe for a bunch charge of $Q = 2\,\text{nC}$ from the linac exit (Fig. 2). Large horizontal dispersion variations appear in the arc regions, while vertical dispersion remains near zero. The R_{56} exceeds 5 m and a peak in $\lambda_{\max}$ near $s \approx 220\,\text{m}$ suggests microbunching onset.

Synchrotron Radiation effects Previous studies on ELEGANT attributed significant emittance growth to ISR and CSR [5], experimental evidence supporting CSR wakefields as the dominant cause of emittance growth was subsequently reported via vertical bump orbit measurements in

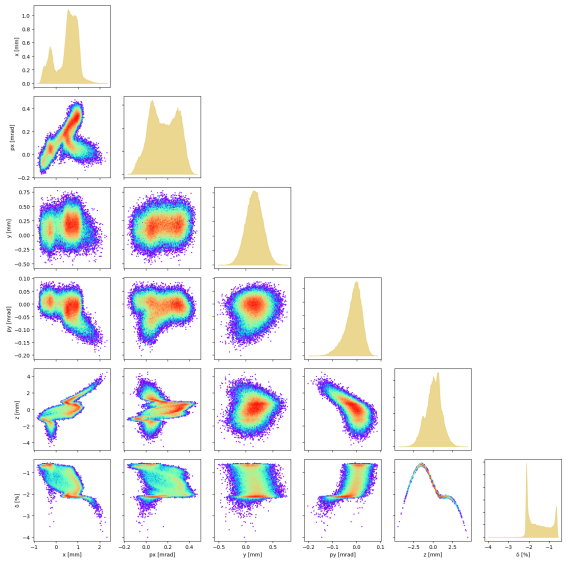

Figure 4: 6D phase space of the electron beam after the J-Arc, including longitudinal and transverse wakefields, misalignments, and CSR.

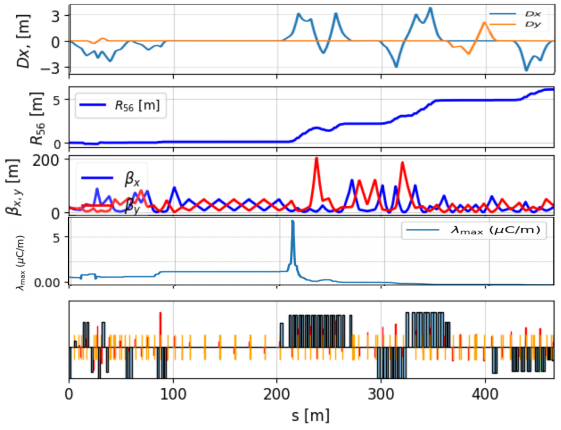

Figure 5: Optical functions and longitudinal beam dynamics along the SuperKEKB BTe beamline simulated with OCELOT for $Q = 2$ nC and RF phase $\phi = 3°$.

the arc sections [11]. We reproduce the ISR contribution in OCELOT by making a dedicated ISR module for dipole magnets, obtaining a horizontal emittance growth of approximately 20 µm rad attributable to ISR alone. For CSR, the previous study reports 50 µm rad [5]; we aim to improve on this by incorporating the realistic dipole vacuum chamber geometry into a 3D CSR calculation, which requires a realistic initial bunch distribution beyond the Gaussian approximation. This motivates the longitudinal phase-space reconstruction at the gun [9], whose output will serve as input to the full CSR study.

Magnetic field imperfections Measured field profiles for each BTe dipole were incorporated into the lattice model, with the near-beam region parameterized by a polynomial fit (Fig. 6), capturing the dominant field curvature. Tracking from the nominal linac output shows negligible emittance growth when only the dipole field shape is included. Including multipole components, however, drives a horizontal emittance increase of approximately 30%, while the vertical emittance remains unaffected.

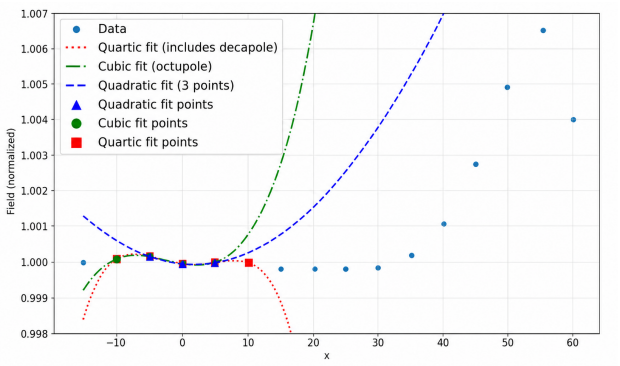

Figure 6: Quadratic fit of the dipole field in the near-beam region.

Table 2: Summary of Horizontal Emittance Growth Contributions in the BTe Line

Effect	$\Delta\gamma\varepsilon_x$ **[µm rad]**
Incoherent synchrotron radiation (ISR)	~20
Coherent synchrotron radiation (CSR)	~50
Dipole magnetic field errors	~10
Total	~90

CONCLUSION

A unified simulation framework for the SuperKEKB injector linac and BTe line has been developed in OCELOT. Space charge, short-range wakefields, ISR, CSR, and dipole field imperfections have been individually quantified. In the BTe line, the dominant contribution to horizontal emittance growth is CSR (~50 µm rad), followed by ISR (~20 μm rad) and dipole field errors (~10 μm rad), totalling ~90 μm rad. Future work will incorporate a realistic initial bunch distribution from ongoing longitudinal phase-space reconstruction at the gun, which will enable a full 3D CSR calculation using the actual BTe vacuum chamber geometry.

REFERENCES

[1] T. Abe *et al.*, "Technical Design Report of SuperKEKB", KEK Report 2010-27, High Energy Accelerator Research Organization, Tsukuba, Japan, 2010.

[2] Y. Ohnishi, "SuperKEKB Luminosity Quest", in *Proc. Int. Workshop on e^+e^- Factories (eeFACT'22)*, Frascati, Italy, Nov. 2022, pp. 1–5. doi:10.18429/JACoW-eeFACT2022-MOXAT0103

[3] Y. Funakoshi *et al.*, "Beam Injection and Beam Quality in Injector LINAC and in Beam Transport Lines at SuperKEKB", *J. Instrum.*, vol. 19, p. T02003, 2024. doi:10.1088/1748-0221/19/02/T02003

[4] N. Iida *et al.*, "Beam injection issues at SuperKEKB", in *Proc. IPAC'23*, Venice, Italy, May 2023, pp. 832–835. doi:10.18429/JACoW-IPAC2023-MOPL120

[5] T. Yoshimoto *et al.*, "Incoherent and Coherent Synchrotron Radiation Effects in the SuperKEKB Electron Beam Transport", in *Proc. 13th Int. Particle Accelerator Conf. (IPAC'23)*, Venice, Italy, May 2023, pp. 295–297. doi:10.18429/JACoW-IPAC2023-MOPA107

[6] I. Agapov *et al.*, "OCELOT: A Software Framework for Synchrotron Light Source and FEL Studies", *Nucl. Instrum. Methods Phys. Res. A*, vol. 768, pp. 151–156, 2014. doi:10.1016/j.nima.2014.09.057

[7] K. Hirata, "An Introduction to SAD", in *Proc. CERN Accelerator School: Frontiers of Particle Beams*, Capri, Italy, Oct. 1988, pp. 62–65. doi:10.5170/CERN-1988-004.62

[8] A. Aguirre Polo, "SAD-to-OCELOT Converter", https://github.com/Andreaaguirrep/SAD-to-OCELOT, 2025.

[9] A. Aguirre *et al.*, "Generative Machine Learning Based Longitudinal Phase Space Reconstruction in KEK Linac Injector", presented at the 6th Workshop on Machine Learning Applications for Particle Accelerators (MaLAPA'26), Himeji, Japan, Apr. 2026.

[10] K. L. F. Bane and M. Sands, "Wakefields of Very Short Bunches in an Accelerating Cavity", *Part. Accel.*, vol. 25, pp. 73–95, 1990. https://cds.cern.ch/record/184288/files/p73.pdf

[11] T. Mori *et al.*, "Vertical Bump Orbit Study on Emittance of Injection Beam in Transport Line for the SuperKEKB Main Ring", in *Proc. 13th Int. Particle Accelerator Conf. (IPAC'23)*, Venice, Italy, May 2023, pp. 298–300. doi:10.18429/JACoW-IPAC2023-MOPA108